



Islamic Azad University



Research Paper

Intermolecular Interaction between Al₁₂N₁₂ Nanocage, Carbon Dioxide and Oxygen Molecules

Soudabeh Abdollahpur¹, Narges Bagheri^{*1}, Mehdi Vadi², Seyed Mohammad Azami³

¹ Department of Chemistry, Firoozabad Branch, Islamic Azad University, Firoozabad, Iran

² Department of Chemistry, Fasa Branch, Islamic Azad University, Fasa, Iran

³ Department of Chemistry, College of Sciences, Yasouj University, Yasouj, Iran

Received: 9 Jun 2022

Revised: 12 Jul. 2022

Accepted: 5 Jul. 2022

Published: 15 Sep 2022

Use your device to scan
and read the article online



Keywords:

Aluminum Nitride,
Intermolecular
Interaction, Attraction,
Repulsion, Electron
Density

Abstract: Adsorption of gaseous molecules on outer surface of nanostructures is one of the interesting properties. In this respect, Al₁₂N₁₂ inorganic system is chosen as nanocage, while oxygen and carbon dioxide are considered to interact with the nanocage. Two modes have been considered in this study. Steric and relaxation deformation densities are employed to find the nature of chemical interaction between these two fragments and results confirm strong steric interaction in the intermolecular area, while the role of relaxation interaction is not negligible. All deformation density calculations for two models of configuration have been investigated using the density functional theory (DFT) calculations by M06-2X methods and 6-311++G** basis set. Interaction energy for two models of molecules has been examined and compared utilizing the method of computation. To get insight into steric and attractive parts of the intermolecular interaction, deformation density is decomposed to two intrinsic components: kinetic energy pressure and relaxation. Competition between these two components has been performed in this research.

Soudabeh Abdollahpur, Narges Bagheri, Mehdi Vadi, Seyed Mohammad Azami.
Intermolecular interaction between Al₁₂N₁₂ nanocage, carbon dioxide and oxygen
molecules. *Journal of Optoelectrical Nanostructures*. 2022; 7 (3): 46- 66

DOI: 10.30495/JOPN.2022.29023.1238

*Corresponding author: Narges Bagheri

Address: Department of Chemistry, Firoozabad Branch, Islamic Azad University,
Firoozabad, Iran. Tell: 00989177035716 Email: nrgs.bagheri@gmail.com

INTRODUCTION

Recently, extensive research has been achieved in the electrical and also optical attributes of some important molecules. [1-6]. Studies of various (XY)_n clusters (X=B, Al, ... and Y=N, P, ...) anticipated the fullerene-like cages X₁₂Y₁₂ has the highest stability. That is, the fullerene-like cages (XY)_n can be considered as magic clusters, with special built-in stability for n=12 [7].

In the last years, a lot of researchers have been focusing on the characterization synthesis, and structural characteristics of nanocages, AlN nanotubes, nanowires, nanosheets. Among of (AlN)_n nanocages, Al₁₂N₁₂ is the most stable structure [8]. There are several reports on BN, AlN, BP and AlP nanocages that can adsorb a variety of molecules on their exterior [9]. Rad and Ayub used DFT calculations to show that guanine molecule can be absorbed on a variety of nanocages exterior [10]. In addition, B₁₂P₁₂ and B₁₂N₁₂ nanoclusters and with Zn and Cu doping have been used for SO₂, CO₂ and COCl₂ adsorption, respectively [11-13]. Furthermore, very recently, Yuki and Chang investigated theoretically on Al₁₂N₁₂ nanocage on the adsorption of HNO as a potential electronic sensor and Φ-type sensor for the detection of HNO [14].

Deformation density, $\Delta\rho$, is a helpful amount in computational chemistry, which can be used to calculate reorganization of charge of a molecule to find out about its chemical properties. By definition, this criterion is the molecular electron densities difference between the complex and the fragments $\rho_{tot} = \rho_{comp} - \rho_{frag}^{(0)}$. There are two ways to examine the deformation density including topological analysis in Cartesian space and orbital analysis as eigenorbitals of deformation density. Total deformation density has been analyzed by several studies and it has become clear how to elicit electronic structure based on deformation density [15-21]. We can explain deformation density as orbital relaxation ($\Delta\rho_{relax}$) components and kinetic energy pressure ($\Delta\rho_{KEP}$) [22-24], so that each has their specific topological characteristics [25-28]. In chemistry, kinetic energy pressure known as steric repulsion effect has been originated from Pauli exclusion principle [29,30]. In addition, relax is generated through electron density redistribution during the intermolecular interaction, which leads to reorganization of orbitals [31]. It is clear that relax deformation density and KEP can be diagonalized, which leads to relative eigenvalues and eigenorbitals when the interaction displaces the charges due intermolecular or intramolecular interaction.

The purpose of the current chore is to conduct a theoretical research of deformation density decomposition into relaxation and steric interactions on intermolecular interaction between (AlN)_n nanocage as a physisorption phenomenon. Thus, a plan was devised to examine the interaction of (AlN)_n

nanocage ($n = 12$) and two diatomic and polyatomic molecules, to shed light into the physisorption in depletion and concentration of electron density language. The following contains a short account of deformation density decomposition into relaxation and steric parts.

COMPUTATIONAL DETAILS

We adopted an $\text{Al}_{12}\text{N}_{12}$ fullerene-like nanocage as adsorbent model. Electronic and geometries ρ -wave functions of $\text{Al}_{12}\text{N}_{12}$ complexes with O_2 and CO_2 , at two different sites were optimized at 6-311++G** [32] and hybrid density functional M06-2X [33] level as basis set in Gaussian (v.09) [34].

In fact, the decomposition of total deformation density (ρ_{tot}) yields two intrinsic components: relaxation deformation densities (ρ_{relax}) and kinetic energy pressure (ρ_{KEP}) to examine the attractive and steric parts of the intermolecular interaction. These three densities are diagonalized to result $\theta_{\Delta,i}^{tot}$, $\theta_{\Delta,i}^{KEP}$ and $\theta_{\Delta,i}^{relax}$ as deformation eigenorbitals, and $n_{\Delta,i}^{tot}$, $n_{\Delta,i}^{KEP}$ and $n_{\Delta,i}^{relax}$ as the corresponding eigenvalues, respectively. Its concentration and depletion parts of each, components have been considered based on eigenvalues sign and yellow and blue colors represent depletion ($\Delta\rho_{depl}$) and concentration ($\Delta\rho_{conc}$) of deformation densities, respectively. Moreover, total eigenvalues of the same sign indicate the total size of charge that is displayed with each deformation density components. Densitizer was used for analyzing deformation density [24,35], eigenorbitals and isosurfaces of deformation densities are plotted in GaussView (v.5.0.8) [36].

It should be noted, kinetic energy pressure (KEP) is pertinent to exchange repulsion [37], which forms among electron pairs with the same spin in interacting molecules. In addition, the intermolecular forces among two molecules with interaction are also performed using electrostatic contributions. The classical interaction of two molecules and static charge distribution yield the first and second order electrostatic interactions. The dispersion and induction effects in the two interacting molecules are caused by the second-order electrostatic contribution [37]. On the Inorganic and biological systems, the dispersion affects the interaction. It happens due to distribution of charges between the interacting molecules, which fluctuates along with the electrons' move. When the electrons enter a configuration of low energy, they become correlated. Especially, dispersion is a key factor in non-polar hydrophobic molecules aggregation in aqueous solution. Therefore, the hydrophobic interactions formed between sites of molecules and carbon nanoring is supported by dispersion in terms of strength.

RESULTS AND DISCUSSION

Deformation density analysis was carried out on intermolecular interaction between Aluminum nitrid nanocage (Al₁₂N₁₂) and some molecules such as oxygen and carbon dioxide gases. Al₁₂N₁₂ is a nanocage that contains 12 nitrogen and 12 aluminum atoms. It should be noted that two kinds of ring have been found in this nanocage; the four-membered rings and also six-membered rings having Th symmetry-, as demonstrated the rings in Fig. 1.

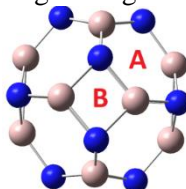


Fig 1. Two kinds of rings, 6-membered rings named A and 4-membered ring named B

The initial orientation of any interacted molecules to the outside surface of Al₁₂N₁₂ nanocage is very important. Indeed, for two kinds of ring in this cage, two models for configuration of O₂ molecule close to the outside surface of Al₁₂N₁₂ nanocage have been considered with respect to six-four member rings. For optimization, various possible initial adsorption geometries via two mentioned rings are considered. In model A, O₂ molecule has been located over the Al and N atoms of the nanocage faced near six-membered ring, as shown in Fig. 2. Another kind of configuration that faces near 4-membered ring named model B, as shown in Fig. 3. Also, two models for CO₂ molecule have been considered such as O₂ molecule.

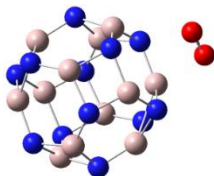


Fig 2. Model A: adsorption of O₂ on the nanocage

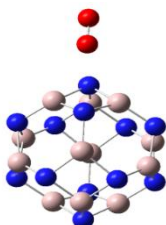


Fig 3. Model B: adsorption of O₂ on the nanocage

O₂ and CO₂ molecules interaction on new surfaces are both important. To find a new surface with good properties was a motivation to us to study the adsorption of the noted molecules. The application of study of Interaction of Al₁₂N₁₂ with O₂ and CO₂ molecules are in medicine and environmental sciences. This kind of interaction of O₂ and CO₂ with nanocages have been subject to different research studies in order to be used in gas sensors as well as devices used for Oxygen storage and removal of poisonous gases.

Geometry optimization and energies have been calculated for the structures prepared. In addition, the frequency of the optimized structures was determined at hybrid density functional M06-2X function with the 6-311++G** basis adopted to regulate a local minimum attendance. The smallest distance of O₂ and CO₂ gases to Al₁₂N₁₂ nanocage is about 2.66 and 2.08 Å in the configurations of model A, respectively. In the model B, the smallest distance of O₂ and CO₂ gases to the nanocage is about 2.59 and 2.08 Å, respectively.

It has been observed that the optimized geometry of Al₁₂N₁₂ nanocage consist of two kinds of non-equivalent bonds of Al-N in a six-membered ring. There are bond lengths of 1.78 and 1.85 Å. However, in the four-membered ring, four AlN bonds are almost equal. This bond length is 1.85 Å.

The interaction energy named as adsorption energy (E_{ads}) is described as follows:

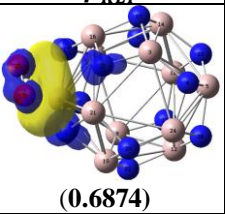
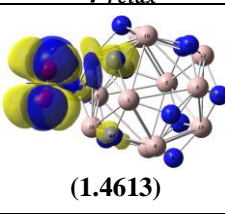
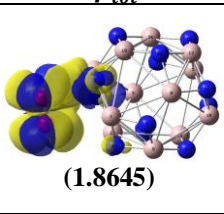
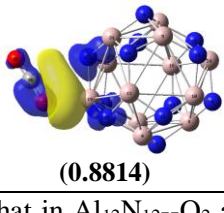
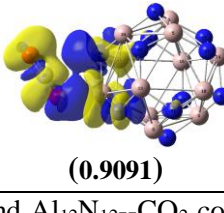
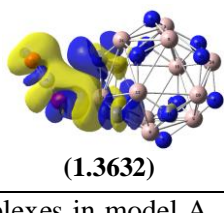
$$E_{ads} = E_{Eadsorbate@nanocage} - E_{adsorbate} - E_{nanocage} \quad (1)$$

Where adsorbate serves as small molecules such as O₂ and CO₂; $E_{(adsorbate@nanocluster)}$ represents the sum of energy of an adsorbate the surface of the nanocage, $E_{(adsorbate)}$ and $E_{(nanocluster)}$ represent the sum of energies of the nanocage and an adsorbate and nanocage, respectively. A negative value of E_{ads} coincides to exothermic adsorption. The energies were computed with the same M06-2X /6-311++G** level of theory.

E_{ad} values between the adsorbate and the adsorbent are -0.0087 and -0.0083 eV for O₂ in model A and B, respectively. For CO₂, E_{ad} values between the adsorbate and the adsorbent are -0.0197 eV in two models, equally. These results clearly indicate that the adsorption between the two species is an exothermic process. Additionally, the results have been shown that the kind of model is not very effective.

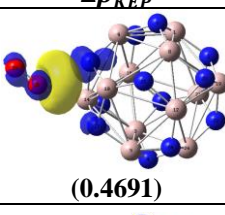
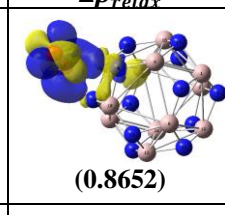
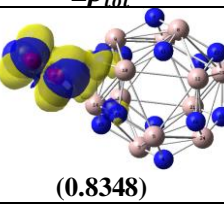
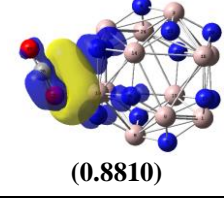
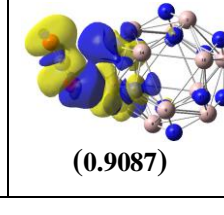
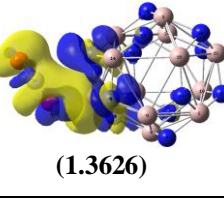
The three-deformation density isosurfaces and displaced charges have been shown in Tables 1 and 2, for complexes of Al₁₂N₁₂ nanocage with Oxygen and Carbon dioxide molecules in model A and B, respectively. As listed in Table 1, the $\Delta\rho_{relax}$ appears mostly in the $\Delta\rho_{tot}$ and the shape of $\Delta\rho_{tot}$ in model A, is completely dominated by $\Delta\rho_{relax}$. Thus, the role of the orbital relaxation is more intensive in total deformation density for these two complexes.

Table 1. Total deformation density isosurface and its corresponding components: kinetic energy pressure and relaxation energy for compounds 1 and 2 as Model A of nano-cage Al₁₂N₁₂ with Oxygen and Carbon dioxide

	Molecule	$\Delta\rho_{KEP}$	$\Delta\rho_{relax}$	$\Delta\rho_{tot}$
1	Al ₁₂ N ₁₂ -O ₂	 (0.6874)	 (1.4613)	 (1.8645)
2	Al ₁₂ N ₁₂ -CO ₂	 (0.8814)	 (0.9091)	 (1.3632)

It is demonstrated that in Al₁₂N₁₂--O₂ and Al₁₂N₁₂--CO₂ complexes in model A, $\Delta\rho_{relax}$ make a wider spread of the deformation density than $\Delta\rho_{KEP}$. Considerably, in Al₁₂N₁₂-O₂ and Al₁₂N₁₂-CO₂ complexes in model B, $\Delta\rho_{relax}$ and $\Delta\rho_{KEP}$ for both O₂ and CO₂ follow the same trend similarly in two complexes as shown in Table 2.

Table 2. Total deformation density isosurface and its corresponding components: kinetic energy pressure and relaxation energy for compounds 1 and 2 as Model B of nano-cage Al₁₂N₁₂ with Oxygen and Carbon dioxide

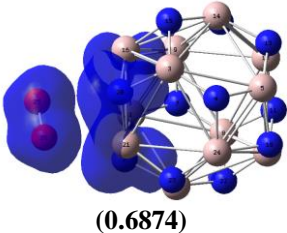
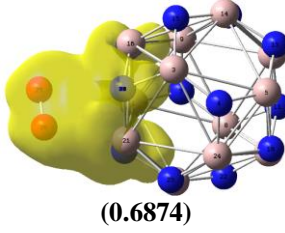
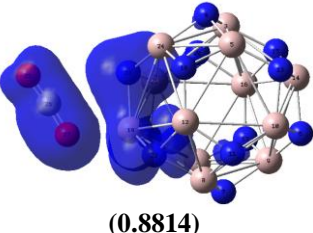
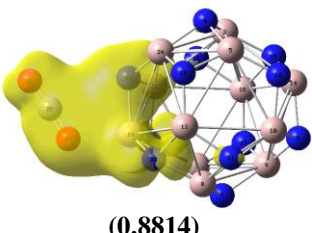
	Molecule	$\Delta\rho_{KEP}$	$\Delta\rho_{relax}$	$\Delta\rho_{tot}$
1	Al ₁₂ N ₁₂ -O ₂	 (0.4691)	 (0.8652)	 (0.8348)
2	Al ₁₂ N ₁₂ -CO ₂	 (0.8810)	 (0.9087)	 (1.3626)

In two models A and B, the displaced charge values due to $\Delta\rho_{relax}$, is higher compared to the corresponding value of $\Delta\rho_{KEP}$ for complexes including O_2 and CO_2 . Thus, compared to the kinetic energy pressure, $n_{\Delta,relax}$ to $n_{\Delta,Total}$ there is a stronger quantitative contribution made by the orbital relaxation to the formation of total deformation density. As to entries in Table 1 and 2, $\Delta\rho_{relax}$ $\Delta\rho_{KEP}$ in $Al_{12}N_{12}-O_2$ and $Al_{12}N_{12}-CO_2$ interactions.

In model A, the values of $n_{\Delta,KEP}$ are compared for the for the complexes. Clearly, this value for CO_2 is higher than that of O_2 . The values of $n_{\Delta,relax}$ for CO_2 are less than O_2 in model A. Moreover, value of $n_{\Delta,KEP}$ is higher than $n_{\Delta,relax}$ in each complex in the two models. About the values of $n_{\Delta,relax}$ and $n_{\Delta,tot}$, it is obvious for two complexes in model A, similarly.

In model B the condition is different from model A. In this model, the values of $n_{\Delta,KEP}$ for the complexes indicate that CO_2 value higher than that of O_2 , Also, the values of $n_{\Delta,relax}$ for CO_2 are more than O_2 . Moreover, the value of $n_{\Delta,KEP}$ is higher than $n_{\Delta,relax}$ in each complex in this model. About the values of $n_{\Delta,tot}$, it is obvious that for CO_2 it is more than O_2 , similarly. Indeed, the trend of $n_{\Delta,relax}$ for O_2 and CO_2 in model A is different from model B.

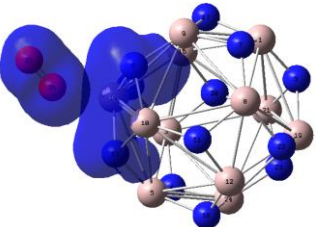
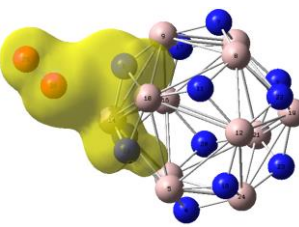
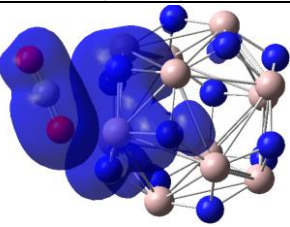
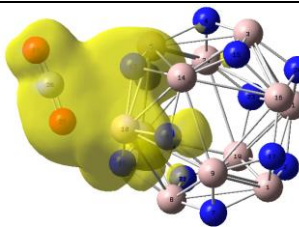
Table 3. Deformation density isosurface of concentration and depletion components of kinetic energy pressure for compounds 1 and 2 as Model A of nano-cage $Al_{12}N_{12}$ with Oxygen and Carbon

	Molecule	$\Delta\rho_{KEP_{conc}}$	$\Delta\rho_{KEP_{depl}}$
1	$Al_{12}N_{12}-O_2$	 (0.6874)	 (0.6874)
2	$Al_{12}N_{12}-CO_2$	 (0.8814)	 (0.8814)

Concentration isosurfaces of ρ_{KEP} for complexes of O_2 and CO_2 with the nanocage in model A have been shown in Table 3. $\Delta\rho_{KEP_{conc}}$ isosurfaces in Table

3 are arranged around the O₂ molecules and the labeled atoms of nanocage near the mentioned molecules such as N2, N17, N20 and Al21 belong to the six-membered ring faced to O₂ molecule in Al₁₂N₁₂--O₂. Also, the same trend has been observed for the atoms N2, N22, N23 and Al19 in Al₁₂N₁₂--CO₂ belong to the six-membered ring separately. However, depletion isosurfaces of ρ_{KEP} for complexes of O₂ and CO₂ with the nanocage ($\Delta\rho_{KEP_{depl}}$) isosurfaces in model A are extended around each atom that is mentioned above in the nanocage besides O₂ and CO₂ molecules continuously. This is not separated from O₂ and CO₂.

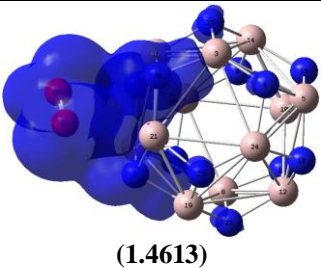
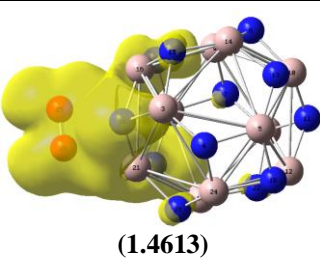
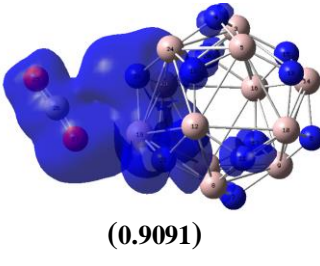
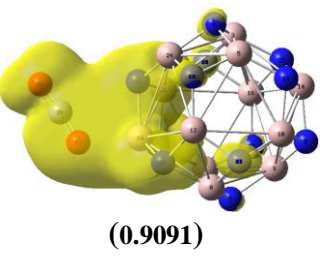
Table 4. Deformation density isosurface of concentration and depletion of kinetic energy pressure for compounds 1 and 2 as Model B of nano-cage Al₁₂N₁₂ with Oxygen and Carbon

	Molecule	$\Delta\rho_{KEP_{conc}}$	$\Delta\rho_{KEP_{depl}}$
1	Al ₁₂ N ₁₂ -O ₂	 (0.4691)	 (0.4691)
2	Al ₁₂ N ₁₂ -CO ₂	 (0.8810)	 (0.8810)

As shown in Table 4, the distribution for $\Delta\rho_{KEP_{depl}}$ isosurfaces for model B is widespread on a wide area of the complexes and the region among these molecules and nanocage. The $\Delta\rho_{KEP_{depl}}$ isosurfaces are focused on O₂ and CO₂ molecules and near atoms of nanocage. However, the $\Delta\rho_{KEP_{conc}}$ isosurfaces are concentrated on O₂ and CO₂ molecules and near atoms separately not continuous. The extension of $\Delta\rho_{KEP_{depl}}$ for Al₁₂N₁₂--CO₂ complex is higher than the Al₁₂N₁₂--O₂ complex and the majority of atoms play a role in the deformation density. The values of $n_{\Delta,KEP}$ for the complexes indicates that CO₂ possesses more $n_{\Delta,KEP}$ value than O₂ in the two models. Also, in Al₁₂N₁₂--CO₂ complex, extension of

$\Delta\rho_{KEP_{conc}}$ is greater than $\text{Al}_{12}\text{N}_{12}\text{-O}_2$ complex and a higher number of atoms are covered by the isosurface between carbon atoms and oxygen molecules (Tables 3 and 4). Therefore, CO_2 can affect the nanocage stronger than O_2 .

Table 5. Deformation density isosurface of concentration and depletion components of relaxation energy pressure for compounds 1 and 2 as Model A of nano-cage $\text{Al}_{12}\text{N}_{12}$ with Oxygen and Carbon

	Molecule	$\Delta\rho_{RLX_{depl}}$	$\Delta\rho_{RLX_{depl}}$
1	$\text{Al}_{12}\text{N}_{12}\text{-O}_2$	 (1.4613)	 (1.4613)
2	$\text{Al}_{12}\text{N}_{12}\text{-CO}_2$	 (0.9091)	 (0.9091)

Tables 5 and 6 reveal the $\Delta\rho_{relax_{conc}}$ isosurfaces are concentrated on a larger number of atoms in the complexes. There is a wide spread of deformation density on wide regions of the molecule and nanocage. As shown by the concentration components of deformation density, all complexes in the two models, it is thoroughly continuous between two fragments in complexes. This continuity for the two models is obvious for relaxation components of deformation density. The depletion and concentration components of relaxation deformation density for $\text{Al}_{12}\text{N}_{12}\text{-O}_2$ in model A show that intermolecular area is affected more by $\text{Al}_{12}\text{N}_{12}\text{-CO}_2$ interactions. The same trend is also shown by values of depletion and concentration. Analysis of the depletion and concentration components of density of relaxation deformation in model B have shown the same trend for two complexes in the aspect of continuity.

In comparison of the values of the components of relaxation deformation density, $\Delta\rho_{relax_{conc}}$ and $\Delta\rho_{relax_{depl}}$, related to two complexes, it has been shown that these values for Al₁₂N₁₂--O₂ are less than Al₁₂N₁₂--CO₂ in model B. This trend differs from the corresponding values for model A.

Tables 7 and 8 illustrate the depletion and concentration of total deformation density have been shown. Clearly, it is the sum ore relaxation and steric interactions. As listed, concentration is mostly located on the molecule and adjacent area, and are spread on other nitrogen and aluminum atoms of nanocage much more than KEP component of mentioned molecules. The value of depletion and concentration components of total deformation density, $\Delta\rho_{relax_{tot}}$ and $\Delta\rho_{relax_{tot}}$, of two complexes in model A for Al₁₂N₁₂--O₂ is more than Al₁₂N₁₂--CO₂ while in model B the values for Al₁₂N₁₂--O₂ is less than Al₁₂N₁₂--O₂.

Table 6. Deformation density isosurface of concentration and depletion components of relaxation energy pressure for compounds 1 and 2 as Model B of nano-cage Al₁₂N₁₂ with Oxygen and Carbon

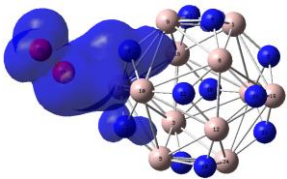
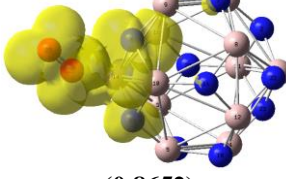
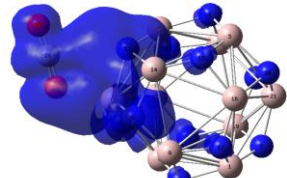
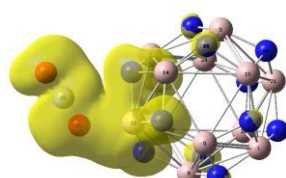
	Molecule	$\Delta\rho_{RLX_{depl}}$	$\Delta\rho_{RLX_{depl}}$
1	Al ₁₂ N ₁₂ -O ₂	 (0.8652)	 (0.8652)
2	Al ₁₂ N ₁₂ -CO ₂	 (0.9087)	 (0.9087)

Table 7. Deformation density isosurface of concentration and depletion components of total energy for compounds 1 and 2 as Model A of nano-cage $Al_{12}N_{12}$ with Oxygen and Carbon

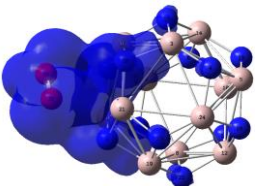
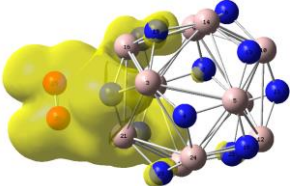
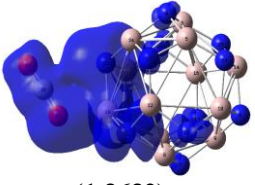
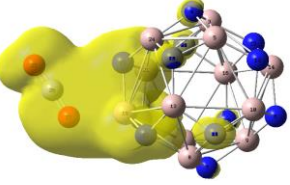
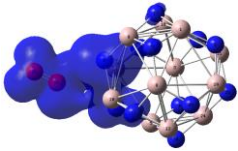
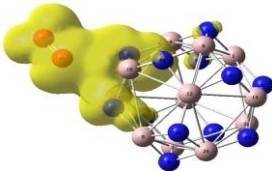
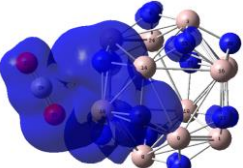
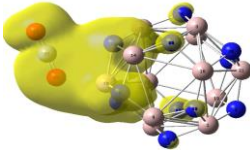
	Molecule	$\Delta\rho_{tot_{conc}}$	$\Delta\rho_{tot_{depl}}$
1	$Al_{12}N_{12}-O_2$	 (1.8645)	 (1.8645)
2	$Al_{12}N_{12}-CO_2$	 (1.3632)	 (1.3632)

Table 8. Deformation density isosurface of concentration and depletion components of total energy for compounds 1 and 2 as Model B of nano-cage $Al_{12}N_{12}$ with Oxygen and Carbon

	Molecule	$\Delta\rho_{tot_{conc}}$	$\Delta\rho_{tot_{depl}}$
1	$Al_{12}N_{12}-O_2$	 (0.8348)	 (0.8348)
2	$Al_{12}N_{12}-CO_2$	 (1.3626)	 (1.3626)

Looking at Tables 3 to 8, there are some considerable points including concentration and depletion isosurfaces of ρ_{KEP} , $\Delta\rho_{relax}$, and $\Delta\rho_{tot}$ for complexes of O₂ and CO₂ with the nanocage, respectively. The deformation density analysis for O₂ and CO₂ molecules indicates that $\Delta\rho_{KEP_{conc}}$ isosurfaces are concentrated near the molecules and the face of nanocage close to the molecule. In other words, not electron density concentration is created by KEP in the intermolecular area. In addition, $\Delta\rho_{KEP_{depl}}$ isosurfaces are concentrated not only near the molecules and the face of nanocage in front of the molecule, but also the deformation density component also affects the intermolecular area. That is, KEP displaces electron density from the intermolecular area. In addition, the depletion component of relaxation deformation density isosurface $\Delta\rho_{relax_{depl}}$ is scattered in intermolecular area. Moreover, the other part of relaxation, $\Delta\rho_{relax_{depl}}$ is continuous and distributed in that region. Tables 7 & 8 the depletion and concentration elements of the whole deformation density and both of them indicate the phenomena illustrated in Tables 5 and 6.

In Table 9 and 10 in the model, to shed more light into deformation eigenorbitals ($\theta_{\Delta,i}$), deformation density, and corresponding eigenvalues because of total, KEP and relaxation contribution represented in models A and B respectively for O₂ and CO₂ molecules in complex with the nanocage. The table includes only five deformation orbitals with significant eigenvalues. The negative and positive values indicate depletion concentration of electron density in the space created by the pertinent orbitals respectively. It is notable that the deformation orbitals for these molecules are shaped in the areas close to the mentioned molecules and the surface of nanocage close to the molecule. Thus, these areas have a higher charge displacement. The θ_{Δ}^{KEP} s that have negative eigenvalues are extended more to the mentioned molecules and positive eigenvalues are extended more to the nanocage. Moreover, θ_{Δ}^{relax} s are expanded in wider areas of both fragments of O₂ and CO₂ molecules and nanocage. For O₂ and CO₂ in complexes, θ_{Δ}^{relax} s indicate the key role of orbital relaxation in the density of total deformation. The general form of deformation orbitals are influenced by θ_{Δ}^{relax} of the molecules. In comparison of two modes, model B represent the deformation orbitals of mentioned molecules in the corresponding and complex eigenvalues because of KEP, total, and relaxation contribution. Similarly, all deformation orbitals of the molecules are formed in close to the noted molecules and the surface of nanoring close the molecule. Relaxation energy component of deformation density controls the effects of this phenomenon; which is illustrated by the pertinent displaced charge component of deformation density. The general forms of the deformation

orbitals are showed by θ_{Δ}^{relax} in these molecules, which is identical to the that noted regarding the O_2 and CO_2 --nanocage complex in model A.

Table 9. KEP, relax and Total highest Molecular Orbitals in model A, for Carbon Nano-Cage O_2 and CO_2 . The respective eigenvalues are represented in parentheses below them.

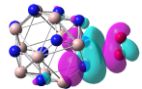
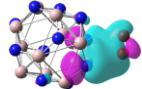
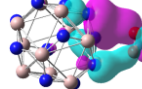
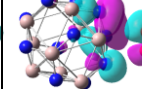
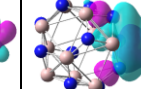
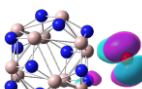
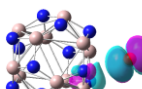

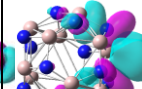
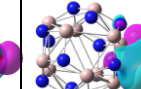
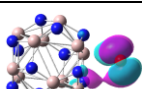
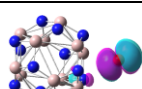
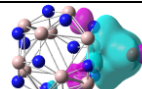
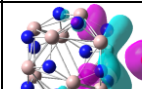
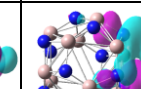
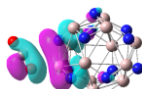
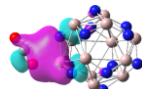
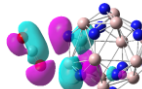
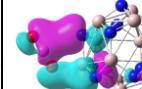
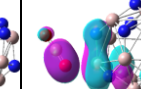
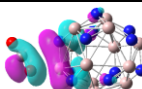
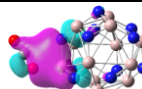
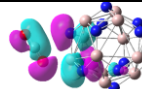
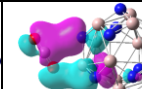
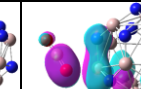
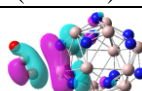
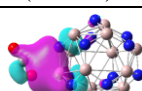
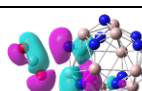
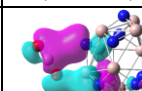
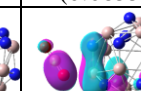
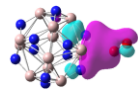
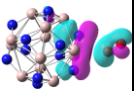
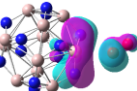
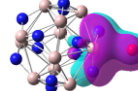
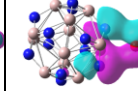
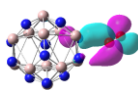
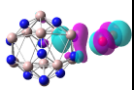
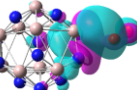
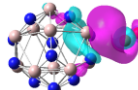
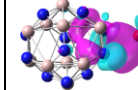
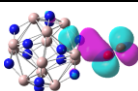
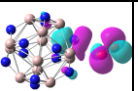
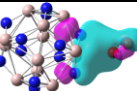
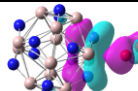
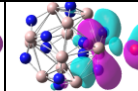
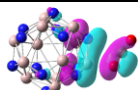
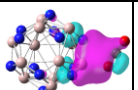
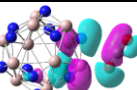
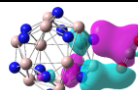
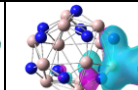
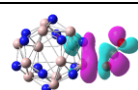
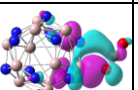
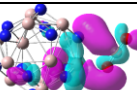
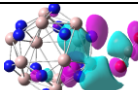
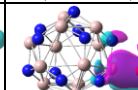
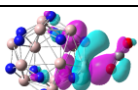
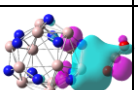
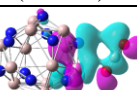
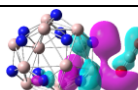
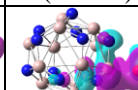
		MO1	MO2	MO3	MO4	MO5
O_2	$\theta_{\Delta,i}^{KEP}$	 (0.3114)	 (-0.3114)	 (-0.1724)	 (0.1724)	 (-0.1177)
	$\theta_{\Delta,i}^{relax}$	 (1.1379)	 (-1.1379)	 (-0.0766)	 (0.0766)	 (0.0353)
	$\theta_{\Delta,i}^{Tot}$	 (1.1569)	 (-1.1082)	 (-0.3065)	 (0.3005)	 (-0.1455)
CO_2	$\theta_{\Delta,i}^{KEP}$	 (0.4323)	 (-0.4323)	 (0.1801)	 (-0.1801)	 (0.1188)
	$\theta_{\Delta,i}^{relax}$	 (-0.2832)	 (0.2832)	 (0.1167)	 (-0.1167)	 (0.0855)
	$\theta_{\Delta,i}^{Tot}$	 (0.5279)	 (-0.04514)	 (-0.2463)	 (0.2219)	 (-0.1527)

Table 10. KEP, relax and Total highest Molecular Orbitals in model B, for Carbon Nano-Cage O₂ and CO₂. The respective eigenvalues are represented in parentheses below them.

		MO1	MO2	MO3	MO4	MO5
O ₂	$\theta_{\Delta,i}^{KE}$	 (-0.3140)	 (0.3140)	 (0.1074)	 (-0.1074)	 (-0.00878)
	$\theta_{\Delta,i}^{rel}$	 (0.5601)	 (-0.5601)	 (0.0805)	 (-0.0805)	 (0.0404)
	$\theta_{\Delta,i}^{To}$	 (0.5959)	 (-0.5959)	 (-0.3023)	 (0.2787)	 (0.1119)
CO ₂	$\theta_{\Delta,i}^{KE}$	 (0.4321)	 (-0.4321)	 (0.1801)	 (-0.1801)	 (-0.1187)
	$\theta_{\Delta,i}^{rel}$	 (-0.2831)	 (0.2831)	 (0.1166)	 (-0.1166)	 (0.0854)
	$\theta_{\Delta,i}^{To}$	 (0.5277)	 (-0.4512)	 (-0.2461)	 (0.2218)	 (-0.1527)

The comparison of our results with other results in literature shows that there is a good agreement with others and our calculations and other observations are in one direction. As we mentioned before about the structure of Al₁₂N₁₂ nanocluster, in according to our computations by M06-2X/6-311++G**, the nanocluster has two diverse bond types: The Al-N bond that is shorter is 1.7843 Å in length in eight 6-membered rings (6MRs), and the longer is 1.8484 Å in length in six 4-membered rings (4MRs). The results indicated that the length of the bonds of the 4MRs are longer than 6MRs to same extent. These results have been compared with other reports. Soltani et al. showed the Al-N bond in Al₁₂N₁₂ nanocluster accompanied by TDOS and ELF plots. They found the Al-N bond in Al₁₂N₁₂

nanocluster 1.849 Å in length in 4MRs and 1.784 Å in 6MRs [38]. Also, Silaghi-Dumitrescu et. al concluded that the bond lengths of the 4MRs are longer than those of the 6MRs [39]. Wang et al. determined the Al–N bond in Al₁₂N₁₂ nanocluster 1.855 Å in length in 4MRs and 1.792 Å in 6MRs [40]. Saeedi et al. found that the optimized structure of Al₁₂N₁₂ nanocluster was 1.874 Å in length in 4MRs and 1.808 Å in 6MRs [41].

CONCLUSION

Deformation density analysis is carried out on interaction between Al₁₂N₁₂ inorganic nanocage and two molecules, oxygen and carbon dioxide in two models, where the chemical phenomenon behind this interaction is adsorption of the corresponding gaseous molecules on the outer wall of nanocage. For mentioned molecules in the two models, kinetic energy relaxation deformation densities and pressure are included and analyzed.

Following analysis of data and surfaces, the findings indicated that the kinetic energy relaxation and pressure are present in different areas. In Al₁₂N₁₂--O₂ and Al₁₂N₁₂--CO₂ complexes, it was shown that orbital relaxation is dominant in total deformation of electron densities. Investigation on depletion and concentration of relaxation, kinetic energy pressure, and total deformation densities indicated that KEP is concentrated close the adsorbed molecule and those atoms of nanocage which are close to the molecule. Furthermore, it is seen that carbondioxide molecule can affect more the nanoring than oxygen. It has been observed that $n_{\Delta,KEP}$ and $n_{\Delta,relax}$ and $n_{\Delta,tot}$ of model A and B for AlN--CO₂ is more than the value for AlN--O₂ expect for $n_{\Delta,relax}$ and of $n_{\Delta,tot}$ of model A is inverse. The value for AlN--O₂ is more than the value for AlN--CO₂. In both models for adsorption of O₂ and CO₂ molecules, $\Delta\rho_{KEP_{conc}}$ is appeared around the adsorbed molecules and nanocage; while $\Delta\rho_{KEP_{depl}}$ isosurfaces are located in wider area. Additionally, it is found that interaction energy as adsorbent energy of Al₁₂N₁₂--O₂ in two models are almost the same.

CONFLICT OF INTEREST

The authors state that publication of this manuscript does not involve any conflicts of interest.

REFERENCES

- [1] T. Niazkar, G. Shams, Z. Soltani. *Electronic, Optical, and Thermoelectric Properties of BaFe_{2-x}Zn_xAs₂(x=0,1,2) orthorhombic Polymorphs: DFT Study*. J. Optoelectron. Nanostructures. 6 (3) (2021) 93-116.
Available: http://jopn.miau.ac.ir/article_4982.html
- [2] S. Damizadeh, M. Nayeri, F. Kalantari Fotooh, S. Fotoohi, *Electronic and Optical Properties of SnGe and SnC Nanoribbons: A First-Principles Study*. J. Optoelectron. Nanostructures. 5(4) (2020) 67-86.
Available: http://jopn.miau.ac.ir/article_4507.html
- [3] M. Mohammadi, M. Vadi, N. Bagheri. *Study of Amitriptyline Drug Adsorption on Multi Walled Carbon Nanotube (MWCNT)*. J. New Materials. 11(43) (2021) 70-81.
Available: http://jnm.miau.ac.ir/article_4679.html?lang=en
- [4] S. J. Mousavi. *Ab-initio LSDA Study of the Electronic States of Nano Scale Layered LaCoO₃/Mn Compound: Hubbard Parameter Optimization*. J. Optoelectron. Nanostructures. 5(4) (2020) 111-122.
Available: http://jopn.miau.ac.ir/article_4512.html
- [5] A. Jahanshir. *Quanto-Relativistic Background of Strong Electron-Electron Interactions in Quantum Dots under magnetic field*. J. Optoelectron. Nanostructures. 6(3) (2021) 93-116.
Available: http://jopn.miau.ac.ir/article_4972.html
- [6] T. Ghaffary, F. Rahimi, Y. Naimi, H. Khajehazad. *Study of the Spin-Orbit Interaction Effects on Energy Levels and the Absorption Coefficients of Spherical Quantum Dot and Quantum Anti-Dot under the Magnetic Field*. J. Optoelectron. Nanostructures. 6(2) (2021) 55-74.
Available: http://jopn.miau.ac.ir/article_4769.html
- [7] F. Younas, M.Y. Mehboob, K. Ayub, R. Hussain, A. Umar, M.U. Khan, Z. Irshad, M. Adnan. *Efficient Cu decorated inorganic B12P12 nanoclusters for sensing toxic COCl₂ gas: a detailed DFT study*. Journal of Computational Biophysics and Chemistry. 20(01) (2021) 85-97.
Available: <https://doi.org/10.1142/S273741652150006X>.
- [8] M. REZAEI SAMETI, H. ZANGANEH. *TD-DFT, NBO, AIM, RDG AND THERMODYNAMIC STUDIES OF INTERACTIONS OF 5-FLUOROURACIL DRUG WITH*

- PRISTINE AND P-DOPED ALI2N12 NANOCAGE*. PHYS. CHEM. RES. 8(3) (2020) 511-527.
Available: <https://www.sid.ir/en/Journal/ViewPaper.aspx?ID=743122>
- [9] M.Y. Mehboob, F. Hussain, R. Hussain, A. Shaikat, Z. Irshad, M. Adnan, A. Khurshid. *Designing of Inorganic AlI2N12 Nanocluster with Fe, Co, Ni, Cu and Zn Metals for Efficient Hydrogen Storage Materials*. Journal of Computational Biophysics and Chemistry. 20(04) (2021) 359-375.
Available: <https://doi.org/10.1142/S2737416521500186>.
- [10] A.S. Meo. 2021. *Environmental Pollution and the Brain*. CRC Press.
Available: <https://www.routledge.com/Environmental-Pollution-and-the-Brain/Meo/p/book/9781032065090>
- [11] S. Hussain, R. Hussain, M.Y. Mehboob, S.A.S. Chatha, A.I. Hussain, A. Umar, M.U. Khan, M. Ahmed, M. Adnan, K. Ayub. *Adsorption of phosgene gas on pristine and copper-decorated B12N12 nanocages: a comparative DFT study*. ACS omega. 5(13) (2020) 7641-7650.
Available: <https://doi.org/10.1021/acsomega.0c00507>.
- [12] M. Adnan, J.K. Lee. *All sequential dip-coating processed perovskite layers from an aqueous lead precursor for high efficiency perovskite solar cells*. Scientific reports. 8(1) (2018) 1-10.
Available: <https://doi.org/10.1038/s41598-018-20296-2>.
- [13] S. Hussain, S.A.S. Chatha, A.I. Hussain, R. Hussain, Y.M. Mehboob, T. Gulzar, A. Mansha, N. Shahzad, K. Ayub, K. *Designing novel Zn-decorated inorganic B12P12 nanoclusters with promising electronic properties: a step forward toward efficient CO2 sensing materials*. ACS omega. 5 (25) (2020) 15547-15556.
Available: <https://doi.org/10.1021/acsomega.0c01686>.
- [14] R. M. Pitzer. *The barrier to internal rotation in ethane*. J. phys. Chem A. 113(45) (2009) 12343-12345. Available: <https://pubs.acs.org/action/doSearch?field1=Contrib&text1=Russell+M.++Pitzer>
- [15] W.H. Schwarz, P. Valtazanos, K. Ruedenberg. *Electron difference densities and chemical bonding*. Theoretica chimica acta. 68(6) (1985) 471-506.
Available: <https://doi.org/10.1007/BF00527670>.

- [16] W.H.E. SCHWARZ, K. RUEDENBERG, L. MENSCHING. *CHEMICAL DEFORMATION DENSITIES. I. PRINCIPLES AND FORMULATION OF QUANTITATIVE DETERMINATION*. J. AM. CHEM. SOC. 111(18) (1989) 6926-6933.
Available: <https://doi.org/10.1021/ja00200a006>.
- [17] T. Gohda, M. Ichikawa, T. Gustafsson, I. Olovsson. *X-ray study of deformation density and spontaneous polarization in ferroelectric NaNO₂*. Acta Cryst. Sec. B: Structural Science. 56(1) (2000) 11-16.
Available: [DOI: 10.1107/s010876819901054x](https://doi.org/10.1107/s010876819901054x).
- [18] G. Will. *Electron deformation density in titanium diboride chemical bonding in TiB₂*. J. Solid State Chem. 177(2) (2004) 628-631.
Available: <https://doi.org/10.1016/j.jssc.2003.04.008>.
- [19] J. Gu, J. Wang, J. Leszczynski. H– Bonding Patterns in the Platinated Guanine– Cytosine Base Pair and Guanine– Cytosine– Guanine– Cytosine Base Tetrad: an Electron Density Deformation Analysis and AIM Study. J. Am. Chem. Soc. 126(39) (2004) 12651-12660.
Available: <https://doi.org/10.1021/ja0492337>.
- [20] F. Ghanavati, S.M. Azami. *Topological analysis of steric and relaxation deformation densities*. Molecular Physics. 115(6) (2017) 743-756.
Available: <https://doi.org/10.1080/00268976.2017.1281457>.
- [21] K. Kiewisch, G. Eickerling, M. Reiher, J. Neugebauer. *Topological analysis of electron densities from Kohn-Sham and subsystem density functional theory*. J. Chem. Phys. 128 (4) (2008) 044114.
Available: <https://doi.org/10.1063/1.2822966>.
- [22] M. Parafiniuk, M.P. Mitoraj. *On the origin of internal rotation in ammonia borane*. J. Mol. Model. 20(6) (2014) 1-9.
Available: [doi: 10.1007/s00894-014-2272-y](https://doi.org/10.1007/s00894-014-2272-y).
- [23] M. P. Mitoraj, M. Parafiniuk, M. Srebro, M. Handzlik, A. Buczek, A. Michalak. *Applications of the ETS-NOCV method in descriptions of chemical reactions*. J Mol Model. 17(9) (2011) 2337-2352.
Available: [DOI: 10.1007/s00894-011-1023-6](https://doi.org/10.1007/s00894-011-1023-6).

- [24] S. Fakhraee, M. Azami. *Orbital representation of kinetic energy pressure*. J. Chem. Phys. 130 (2009) 084113.
Available: <https://doi.org/10.1063/1.3077026>.
- [25] J.T. Su, W.A. Goddard. *The dynamics of highly excited electronic systems: Applications of the electron force field*. J. Chem. Phys. 131 (2009) 244501.
Available: <https://doi.org/10.1063/1.3272671>.
- [26] K. Ruedenberg. *The Physical Nature of the Chemical Bond*, Rev. Mod. Phys. 34 (1962) 326.
Available: <https://doi.org/10.1103/RevModPhys.34.326>
- [27] H. Tokiwa, H. Ichikawa. *Origin of steric hindrance in ethane*. Int. J. Quant. Chem. 50 (2) (1994) 109-112.
Available: <https://onlinelibrary.wiley.com/doi/abs/10.1002/qua.560500204>
- [28] S.G. Wang, Y. X. Qiu, W.H.E. Schwarz. *Bonding or Nonbonding? Description or Explanation? "Confinement Bonding" of He@adamantane*, chemistry A European journal. 15(24) (2009) 6032-6040.
Available: <https://doi.org/10.1002/chem.200802596>.
- [29] V. Weissopf. *Of Atoms, Mountains, and Stars: A Study in Qualitative Physics*. SCIENCE. 187 (4177) (1975) 605-612.
Available: <https://www.science.org/doi/10.1126/science.187.4177.6>.
- [30] F. Weinhold and C.R. Landis, *Valency and bonding: a natural bond orbital donor-acceptor perspective* (Cambridge University Press, Cambridge, p 37, 2003).
Available:
https://scholar.google.com/scholar?q=F.+Weinhold+and+C.R.+Landis,+Valency+and+bonding:&hl=fa&as_sdt=0&as_vis=1&oi=scholart
- [31] A.I. Ermakov, A.E. Merkulov, A.A. Svechnikova. *Basis Set Orbital Relaxation in Atomic and Molecular Hydrogen Systems*. J. Struct. Chem. 45(6) (2004) 923-928.
Available: DOI:[10.1007/s10947-005-0080-z](https://doi.org/10.1007/s10947-005-0080-z)
- [32] A.D. Mclean. *Contracted Gaussian basis sets for molecular calculations. I. Second row atoms, Z=11-18*. J. Chem. Phys. 72 (1980) 5639.
Available: <https://doi.org/10.1063/1.438980>.

- [33] Y. Zhao, D.G. Truhlar. The M06 suite of density functionals for main group thermochemistry, thermochemical kinetics, noncovalent interactions, excited states, and transition elements: two new functionals and systematic testing of four M06-class functionals and 12 other functionals. *Theor. Chem. Accounts*. 120 (2008) 215-241. Available: <https://doi.org/10.1007/s00214-007-0310-x>.
- [34] M. J. Frisch, G. W. Trucks, H. B. Schlegel et al., Gaussian 09, revision A.02. Gaussian Inc, Pittsburgh, PA, 2009. Available: www.gaussian.com
- [35] S.M. Azami, Densitizer Ver. 1.1.48 (<http://densitizer.orbital.xyz>), 2019. Available: <http://densitizer.orbital.xyz>
- [36] Gaussian, Inc (2000-2008) GaussView 5.0. Gaussian, Inc. copyright (c) Semichem, Inc. Available: www.gaussian.com
- [37] A. J. Stone, The theory of intermolecular forces. (Oxford University Press, Oxford.1996). Available: <https://oxford.universitypressscholarship.com/view/10.1093/acprof:oso/9780199672394.001.0001/acprof-9780199672394>
- [38] S. Sedighi, M. T. Baei, M. Javan, J. C. Ince, A. Soltani, M.H. Jokar, S. Tavassoli. *Adsorption of sarin and chlorosarin onto the Al₁₂N₁₂ and Al₁₂P₁₂ nanoclusters: DFT and TDDFT calculations*. *Surf Interface Anal.* 52(11) (2020) 725-734. Available: <https://onlinelibrary.wiley.com/doi/abs/10.1002/sia.6861>
- [39] I. Silaghi-Dumitrescu, F. Lara-Ochoa, I. Haiduc. *Al₂B₁₂ (A = B, Al; B = N, P) fullerene-like cages and their hydrogenated forms stabilized by exohedral bonds. An AM1 molecular orbital study*. *J. Mol. Struct. (THEOCHEM)*. 370(1) (1996) 17-23. Available: <https://fddocuments.in/document/a12b12-a-bal-b-np-46-fullerene-like-cages-and-their-hydrogenated-forms.html>
- [40] Q. Wang, Q. Sun, P. Jena, Y. Kawazoe. *Potential of AlN nanostructures as hydrogen storage materials*. *ACS Nano*. 3(3) (2009, March) 621-626. Available: <https://doi.org/10.1021/nn800815e>

- [41] M. Saeedi, M. Anafcheh, R. Ghafouri, N.L. HadipourL. *A computational investigation of the electronic properties of Octahedral Al_nN_n and Al_nP_n cages (n = 12, 16, 28, 36, and 48)*. Struct Chem. 24(2) (2013) 681-689. Available: <https://link.springer.com/article/10.1007/s11224-012-0119-7> .